

Article

Dual-Functional Nanostructures for Purification of Water in Severe Conditions from Heavy Metals and *E. coli* Bacteria

Abdulaziz Abdulrahman AMulla ^{1,*}, Osama Saber ², Mohamed Farouk Ezzeldin ¹,
Mahmoud Mohamed Berekaa ¹ and Waleed I. M. El-Azab ³

¹ Department of Environmental Health, College of Public Health, Imam Abdulrahman Bin Faisal University (IAU), P.O. Box 1982, Dammam 31441, Saudi Arabia

² Department of Physics, College of Science, King Faisal University, P.O. Box 400, Al-Ahsa 31982, Saudi Arabia

³ Egyptian Petroleum Research Institute, Nasr City, P.O. Box 11727, Cairo 11765, Egypt

* Correspondence: aaamulla@iau.edu.sa

Abstract: Because of industrial water, many groundwater sources and other water bodies have a strongly acidic medium. Increased bacterial resistance against multiple antibiotics is one of the main challenges for the scientific society, especially those commonly found in wastewater. Special requirements and materials are needed to work with these severe conditions and treat this kind of water. In this trend, nanolayered structures were prepared and modified in different ways to obtain an optimum material for removing different kinds of heavy metals from water in severe conditions, alongside purifying water from a Gram-negative bacteria (*E. coli*), which is an indication for fecal pollution. An ultrasonic technique effectively achieved this dual target by producing nanolayered structures looking like nanotapes with dimensions of 25 nm. The maximum removal percentages of the heavy metals studied (i.e., iron (Fe), copper (Cu), chromium (Cr), nickel (Ni), and manganese (Mn)) were 85%, 79%, 68%, 63%, and 61%, respectively for one prepared structure. In addition, this nanostructure showed higher antimicrobial activity against the most common coliform bacterium, *E. coli* (inhibition zone up to 18.5 mm). This study introduces dual-functional material for removing different kinds of heavy metals from water in severe conditions and for treating wastewater for Gram-negative bacteria (*E. coli*).

Keywords: ultrasonic technique; layered double hydroxides; removal efficiencies; iron; copper; chromium; nickel; manganese; antimicrobial activity; wastewater treatment



Citation: AMulla, A.A.; Saber, O.; Ezzeldin, M.F.; Berekaa, M.M.; El-Azab, W.I.M. Dual-Functional Nanostructures for Purification of Water in Severe Conditions from Heavy Metals and *E. coli* Bacteria. *Water* **2022**, *14*, 3010. <https://doi.org/10.3390/w14193010>

Academic Editor: Alexandre T. Paulino

Received: 16 July 2022

Accepted: 22 September 2022

Published: 24 September 2022

Publisher's Note: MDPI stays neutral with regard to jurisdictional claims in published maps and institutional affiliations.



Copyright: © 2022 by the authors. Licensee MDPI, Basel, Switzerland. This article is an open access article distributed under the terms and conditions of the Creative Commons Attribution (CC BY) license (<https://creativecommons.org/licenses/by/4.0/>).

1. Introduction

There is no doubt that pollutants, heavy metals, and bacteria can damage the human body's bone, liver, kidney, gastrointestinal system, and nerves and deactivate the functional groups of important enzymes [1–3]. According to the Environmental Protection Agency (EPA), the limit values for iron (Fe), copper (Cu), chromium (Cr), nickel (Ni), and manganese (Mn) ions in drinking water are 0.3, 1.0, 0.1, 0.1, and 0.05 mg/L, respectively [3,4]. Hence, industrial discharges must be treated to protect human health, groundwater sources, and other receiving water bodies from contamination. Generally, few water and wastewater treatment techniques have been established [1] (e.g., precipitation and coagulation, electro dialysis, ion exchange, and adsorption). Even for treated wastewater for agriculture purposes, the Saudi Ministry of Municipal, Rural Affairs, and Housing declared maximum limit values for the occurrence of heavy metals in the reuse of tertiary-treated wastewater for agriculture purposes. For example, the limit concentrations of Fe, Cu, Cr, Ni, and Mn are 5.0, 0.4, 0.1, 0.2, and 0.2 mg/L, respectively [5]. Several approaches have been established to choose a specific water and wastewater treatment technique depending on the concentrations of cations and anions, water source, eco-friendly availability, and treatment cost [1]. Nowadays, wide applications of nanomaterials in different fields have been recognized

and reported by many scientists. These promising structures have been successfully used as removal agents of pollutants [6], catalysts in industries [7], drug delivery vehicles [8], sensing agents [9], and in biological applications [10] due to their small sizes, which mean large specific surface areas and strong adsorption capacities and reactivity. Additionally, one more criterion is well-known: the high mobility of nanomaterials in solutions [11].

Indeed, applying nanomaterials in water and wastewater treatment is one of the rapidly growing fields of science. Different nanostructures have been generated for water purification, such as nanolayered material, nanohybrids, carbon nanotubes, and nanocomposites [12]. Many studies about the removal or partial removal of heavy metals [13], organic pollutants [14], inorganic anions [15,16], and bacteria deactivation [17] using nanomaterials have been published.

Layered double hydroxides (LDHs) can be defined as anionic clays, basic types of hydroxalite-like compounds. Various advantages of LDHs were described, such as high resistance to changes in pH and temperature of the medium, high surface area, memory effect properties, and high capacity of anion exchange treatments, as well as low cost for production [18]. Although of all these are great features, practical applications of pure LDHs are limited. Large charge density and high hydrophilic properties are known as disadvantages of using LDHs in significant industrial applications. One of the main reasons for this restriction is their low tendency to interact with compounds of hydrophobic linkages and compose intramolecular structures with high aggregation properties [19]. Consequently, the need to develop pure LDH structure to overcome these weaknesses can be achieved through interaction with adjusting agents or the consideration of new preparation methods. Both organic and inorganic modifiers may be used to treat the surface and interlayer spaces of LDHs for modification purposes [20].

The manufacture of LDHs usually depends on using an extended range of divalent or trivalent cations accompanied by various interlayer anions [19]. However, many factors should be considered when synthesizing such an LDH structure is required. For example, the method of preparation, characters of interlayer anions, metallic cations, morphological properties, and crystalline structure are the most important aspects [21]. Consequently, the produced LDH materials gain different physical characteristics, leading to distinct industrial applications. Many fabrication methods have been issued for the production of several kinds of LDHs. The most common methods may be summarized as coprecipitation, anion exchange, hydrothermal methods, urea hydrolysis, microwave methods, and sol-gel methods. Nevertheless, the coprecipitation process accompanied by irradiation-applying ultrasound technology has been considered a promising technique for developing innovative LDH materials with new properties, as has been presented in previous studies [22–24]. The environmentally friendly, time-consuming, economic production of uniformly dispersed LDH structures is a prominent feature in the production of LDHs through the sonication process [25,26].

Recently, many studies have been published in the field of remediation of different pollutants from water and wastewater using developed LDH structures. These reports have been devoted to eliminating organic [27,28] and inorganic pollutants in water [29–31]. However, further research is needed to improve the synthesis and final characteristics of LDHs to maximize the removal of water and wastewater pollutants. Hence, the current study aims to address new modified LDH materials capable of significantly removing several heavy metals from water with low pH values. In addition, the lethal effect of nanomaterials on Gram-negative coliform bacteria (*E. coli*) commonly associated with fecal pollution is closely investigated. To achieve these goals, a series of modifications are applied to developing new nanolayered structures of LDHs. The ultrasonic technique is used to modify the platelets' sizes and the layers of LDHs. Moreover, the nanolayered structure of LDHs is modified by changing the percentage of inorganic metals of di- and trivalent metals inside LDHs. Finally, the newly modified nanolayered structures are tested for possible application in water purification to eliminate some heavy metals and the coliform bacterium *E. coli*.

2. Materials and Methods

2.1. Preparation of Nanolayered Structures

Three samples of Al/Zn nanolayered materials were prepared and modified with different techniques. A standard sample was prepared using urea hydrolysis through reacting an aqueous solution (0.049 mol) of zinc nitrate with (0.021 mol) aluminum nitrate. In this reaction, urea (0.5 mol) was added and used as a pH controller. In addition, 0.5 g of polyvinyl alcohol was used in the reaction as a binder. The reaction was carried out at 90 °C for 12 h to obtain a white residue. The sample was filtrated and washed with deionized water several times. After drying at room temperature, the white powder was collected and coded under ZA-1. By decreasing the content of aluminum, the nanolayered structure was modified to produce a new sample, ZA-2. ZA-2 was prepared by reacting 0.059 mol of zinc nitrate with 0.0105 mol of aluminum nitrate in the presence of 0.5 mol of urea. Under the same conditions, a white powder of ZA-2 was collected. The sample ZA-3 was prepared using the same procedure as standard sample ZA-1 and modified using an ultrasonic technique. The ultrasonic technique was used to modify the precipitation process of the product. The temperature of the reaction in all the preparations was kept at 90 °C. The products were washed with distilled water. They were dehydrated at room temperature for 48 h.

2.2. Characterization Techniques

X-ray diffraction (XRD) is considered one of the main tools for determining nanolayered structures. The X-ray diffraction technique (Bruker-AXS, Karlsruhe, Germany) used wide-angle x-ray scattering over $2\theta = 4^\circ$ to 50° in steps of 0.1° or 0.02° with Cu-K α radiation ($\lambda = 0.154$ nm). Transmission electron microscopy (TEM) was used to observe the shapes and sizes of the LDHs. The powder was dispersed in a solvent, coated deeply on a carbon filmed grid in the solution, and left to evaporate the solvent. Then, the sample was ready for TEM measurement. TEM was carried out at room temperature using a JEM 2100F instrument (JEOL Company, Tokyo, Japan) operating at 200 kV. Energy-dispersive X-ray spectroscopy (EDX) is an analytical technique used to identify the compositions of solid materials. EDX measurements were carried out using a JED 2300 Electron Probe Micro analyzer (JEOL Company, Tokyo, Japan) operating up to 10.5 Kev. The thermal analyses consisted of thermal gravimetric analysis (TGA) and differential scanning calorimetry (DSC). The TGA was carried out with a TA thermogravimetric analyzer (series Q500) (TA Company, New Castle, PA, USA), which was used to characterize the decomposition and thermal stability of materials under a nitrogen flow of 30 mL/min with a heating rate of $10^\circ\text{C min}^{-1}$ up to a maximum temperature of 600 °C. The DSC analysis was carried out using a TA series Q 600 (TA Company, New Castle, PA, USA) under a flow of nitrogen of 30 mL/min with a heating rate of $10^\circ\text{C min}^{-1}$ up to a maximum temperature of 600 °C.

2.3. Adsorption Experiment

The removal efficiencies (REs; %) of the modified structures, alongside Greensand PlusTM, were investigated at room temperature (24 °C). Greensand Plus was used as a model of real commercial material at markets for comparison. Greensand Plus is a common filter for removing iron, manganese, hydrogen sulfide, and arsenic for many commercial and industrial water treatment plants. It is also branded as a black filter, and it is mainly composed of silica sand as a support material, coated with fused manganese dioxide. Water treatment with this saleable media is a catalytic oxidation–reduction reaction of Fe and Mn in applied water.

A weight (g) of the prepared nanomaterial was stirred in a volume (L) (i.e., a ratio of w/v ; 2 g/L) of freshly prepared multi-element standard solution containing some interesting heavy metals (Fe, Cu, Cr, Ni, and Mn) at pH 2–3 for up to 1 h. The metal concentrations were chosen to reflect the estimated value of agriculture wastewater before treatment [5] and those that might arise in the future. After equilibrium (1 h), the suspension was separated by centrifugation. Then, the residual concentrations of heavy metals were determined

using different optimized wavelengths of the measured metals with an inductively coupled plasma-optical emission spectrophotometer (ICP-OES). Removal efficiency (RE; %) was calculated using the following formula:

$$\text{RE (\%)} = (C_i - C_f) / C_i \times 100$$

where C_i and C_f (mg/L) are the initial and final concentrations of ions, respectively.

2.4. Antimicrobial Activity

Bacterial strain and media: To test the antimicrobial effect of surface-modified Zn-Al LDH nanomaterial, the most common coliform bacterium in wastewater, namely *E. coli*, was brought from a culture collection from the College of Medicine, Imam Abdulrahman Bin Faisal University (University of Dammam), Saudi Arabia. A nutrient agar medium (OXOID, Hampshire, England) was used to support microbial growth. In contrast, a diagnostic sensitivity agar medium (HIMEDIA, Thane West, India) was used to test the possible antimicrobial effect.

Antimicrobial inhibition test through agar diffusion method: To test the antimicrobial activities of the different nanostructures, a defined weight of each material was sterilized through exposure to UV radiation for 3 min and subsequently dissolved in water (5–25 mg/mL) or dimethyl sulfoxide (DMSO) (10 mg/mL). For antimicrobial activity, the modified agar diffusion method was used [32]. In this method, a thin film of *E. coli* bacteria was spread on the surface of the diagnostic sensitivity agar medium using a cotton swab. Afterward, 100 μ L of nanomaterial was placed in pores approximately 6 mm in diameter. Subsequently, plates were incubated at 37 °C for 24 h. At the end of the incubation period, plates were examined for the existence of an inhibition zone (measured with an accuracy of 0.5 mm in two perpendicular locations). The results were expressed as the mean zone of inhibition in mm \pm standard deviation beyond the standard well diameter (6 mm).

3. Results

3.1. Effect of Al/Zn Nanolayered Structures on Heavy Metal Removal

X-ray diffraction (XRD) was used to characterize the crystal size and layered structure of the prepared Al/Zn LDHs. The XRD pattern of the ZA-1 sample agreed with natural hydroxylated layered structure (JCPDS file 37-629) and synthetic Zn-Al LDH (JCPDS file 48-1022), as shown in Figure 1a.

It exhibited a sharp reflection for the basal plane (003) at $d = 0.76$ nm. Additionally, the reflections of planes (006) and (009) were clear at $d = 0.38$ nm and $d = 0.26$ nm, respectively. The clear arrangement between these values matching with successive diffractions by basal planes, i.e., $d(003) = 2d(006) = 3d(009)$ for ZA-1, revealed highly ordered nanolayers along axis c . The value c , related to the thickness of the brucite-like layer and the interlayer distance, was calculated as three times the interlayered spacing of plane (003), i.e., 2.28 nm. The c dimension was identical to that reported for the natural and synthetic hydroxylated at 2.28 nm.

By reducing the percentage of aluminum, the second sample, ZA-2, was formed. The XRD pattern of the ZA-2 sample showed no shifting in parameter (c) of the nanolayered structure, as shown in Figure 1. In addition, a new phase of zinc hydroxyl carbonate was observed, which agreed with the peak observed at 0.67 nm. It means that sample ZA-2 had a lower percentage of nanolayered structures than ZA-1.

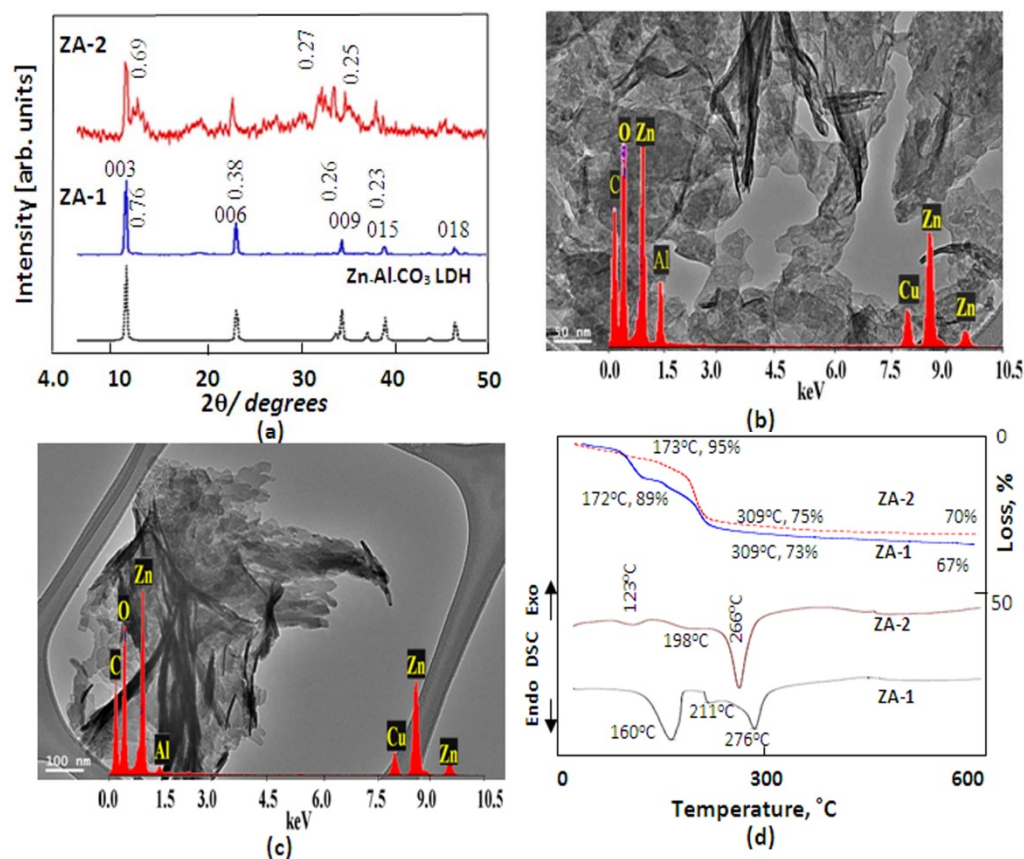


Figure 1. Samples ZA-1 and ZA-2: (a) X-ray diffraction (b,c); TEM images and EDX spectra; and (d) thermal analyses.

Natural samples of layered double hydroxide (pyroaurite) exhibit plate-like morphologies with plates being millimeters in thickness and centimeters in width [30]. In addition, it is known that hydrotalcite crystals possess hexagonal, plated morphologies if carefully crystallized [33]. A similar morphology was observed for ZA-1, with a dimension of plates in the order of 100 nm, as shown in Figure 1b. The analysis of energy-dispersive X-ray spectrometry revealed that zinc, aluminum, carbon, copper, and oxygen were identified in the platelets of sample ZA-1, as shown in Figure 1b (inset). It should be mentioned that the Cu and C signals were attributed to the carbon-coated copper grid of the TEM testing. In the case of sample ZA-2, which had a low concentration of aluminum, TEM images showed irregular plates and shapes, as shown in Figure 1c, agreeing with XRD results. The low concentration of aluminum in sample ZA-2 was confirmed by the intensity of the aluminum peaks in the EDX spectra, as shown in Figure 1c (inset).

Thermal measurements were used to investigate the phase transformations of the samples during the thermal treatment. The recorded thermograms (thermogravimetric, TG) and differential scanning calorimetric (DSC) curves (Figure 1d) showed that the degradation occurred in several stages with various mass rate losses, depending upon the nature of the interlayer anions. As shown from the TG curves of ZA-1, the degradation process exhibited four weight losses, as shown in Figure 1d. The first mass loss (12 wt.%) was detected at a temperature of 170 °C, which could be contributed to loss in both physisorbed and interlayer water. The other three mass losses (16 wt.%) were observed at higher temperatures (170–310 °C). These transitions could be attributed to the decomposition of cyanate and carbonate anions that was confirmed from the FT-IR spectrum, in addition to the dehydroxylation process. Compared with ZA-1, the TG curve of ZA-2 was a little different because the amount of the interlayered water decreased to be 5 wt.% observed at 161 °C, indicating a lowering in the nanolayered structure of LDH. Additionally, the total

weight loss decreased to 26 wt.%. The decomposition of carbonate and cyanate anions was observed in the range of 161–310 °C, as shown in Figure 1d.

To determine the ability of the prepared materials, ZA-1 and ZA-2, to purify water from heavy metals, adsorption experiments were performed for an aqueous standard solution containing iron (Fe), copper (Cu), chromium (Cr), nickel (Ni), and manganese (Mn) with an extremely acidic medium (pH 2~3). The initial concentrations of the analyzed standards are reported in Table 1.

Table 1. Initial concentrations of some heavy metals in the analyzed mixed standard.

Heavy Metal	Concentration (mg/L)
Iron (Fe)	17.7
Copper (Cu)	18.7
Chromium (Cr)	18.2
Nickel (Ni)	14.4
Manganese (Mn)	20.2

Using ZA-1 as an adsorbent, the maximum removal percentages of Fe, Cu, Cr, Ni, and Mn were 66%, 15%, 25%, 4%, and 3%, respectively, as shown in Figure 2. The high removal of Fe by ZA-1 could be explained according to its nanolayered structure because the removal percentage of Fe decreased from 66% to 43% in the case of using sample ZA-2, which had a low nanolayered structure. In addition, this behavior was similar to the removal of other heavy metals. For copper and chromium, the REs decreased to 8% and 3%, respectively. In the same trend, no removal was observed for nickel or manganese.

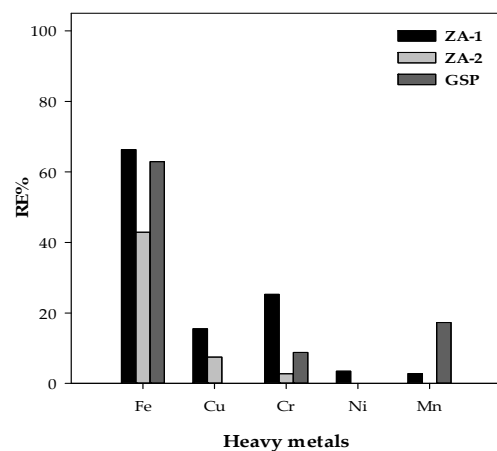


Figure 2. The removal percentages of heavy metals from water at an extremely acidic medium for samples ZA-1, ZA-2, and Greensand Plus (GSP).

According to the X-ray diffraction calculations and the nanolayer size (0.48 nm), we can suggest that the interlayered spacing of the nanolayered structures at 0.28 nm was suitable and favorable for trapping and confining iron particles among the nanolayers, as shown in Figure 3.

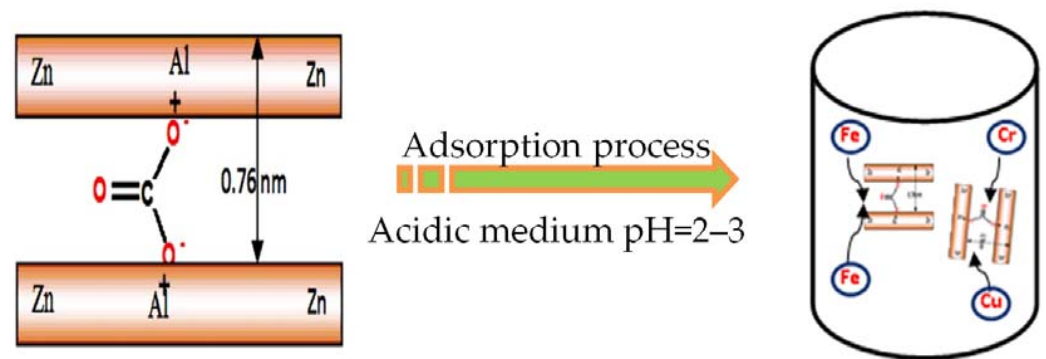


Figure 3. Adsorption process for purifying water from heavy metals in an extremely acidic medium.

One can understand that the optimum operation conditions for effective Greensand filtration were feeding naturally neutral water or neutralized water—most likely at pH of 6.7 to 8.8—and the total concentration of both Fe and Mn combined preferably to be less than 15 ppm in feed water. The current study counted as a kind of severe water treatment condition. Although the pH was extremely acidic—pH 2~3—alongside numerous concentrations of many heavy metals, which were about 90 ppm (total concentration of Fe and Mn combined was about 40 ppm), as shown in Table 1, the tested prepared materials and Greensand Plus were still able to resist these conditions without breakdown.

The REs achieved by Greensand Plus were 62%, 18%, and 9% for Fe, Mn, and Cr, respectively, whereas no adsorption was noticed for Cu and Ni. Compared with the results of Greensand Plus, the prepared sample of ZA-1 was more favorable and useful than Greensand Plus for removing iron and chromium, as seen in Figure 2.

3.2. Effect of Ultrasonic Technique on the Ability of Nanolayered Structures for Heavy Metal Removal

According to many reports [1–3], ultrasound energy can cause physical and chemical changes to structures of materials during their preparation because of the breakdown of cavitation bubbles in the liquid system.

In our study, the ultrasonic technique was used to modify and develop the sizes and nanolayered structures of Al/Zn LDHs by preparing sample ZA-3. X-ray diffraction of ZA-3 showed sharp peaks at low angles and weak peaks at high angles, agreeing with the nanolayered structures, as seen in Figure 3. Sharp peaks were observed at $2\theta = 11.71^\circ$ and 23.41° , agreeing with d-spacing at 0.754 nm and 0.379 nm, respectively. Weak peaks were exhibited at $2\theta = 34.60^\circ$, 39.16° , and 47.21° , agreeing with d-spacing at 0.253 nm, 0.230 nm, and 0.195 nm, respectively. Figure 4 showed that the first three symmetric peaks, which were due to the basal (003), (006), and (009) planes, confirmed the good arrangement of the successive diffraction of their planes, i.e., $0.754 \text{ nm} = 2 \times 0.379 \text{ nm} = 3 \times 0.253 \text{ nm}$. The two asymmetric peaks observed at 0.230 nm and 0.195 nm belonged to the nonbasal (015) and (018) planes. Compared to hydrotalcite-like material (JCPDS file 37-629) and synthetic Zn/Al LDH (JCPDS file 48-1022), sample ZA-3 had a nanolayered structure of zinc aluminum hydroxide carbonate hydrate.

Figure 4a revealed a weak peak appearing at $2\theta = 19.4^\circ$ (d-spacing = 0.456 nm) corresponding to the reflection of 101 planes of polyvinyl alcohol, which was used as a binder during the building of the nanolayered structure [4]. In addition, very weak peaks were observed at $2\theta = 12.96^\circ$, 26.79° , and 36.80° , agreeing with the hydrozincite phase $\text{Zn}_5(\text{OH})_6(\text{CO}_3)_2$ (JCPDS file 72-1100). It means that the nanolayered structure of ZA-3 had traces of the hydrozincite phase.

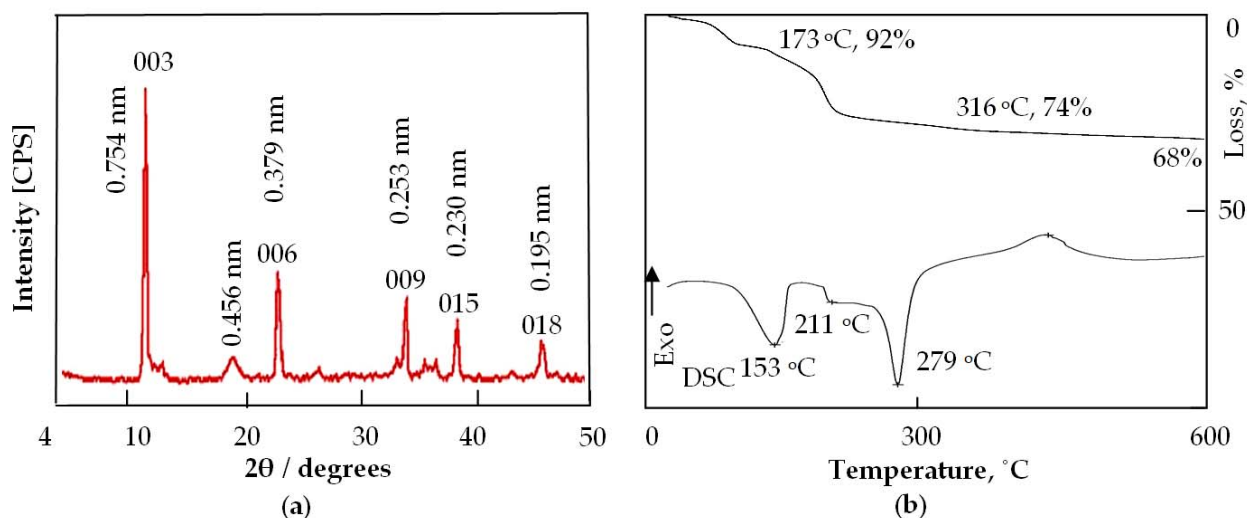


Figure 4. Sample ZA-3: (a) X-ray diffraction and (b) thermal analyses.

Thermal analyses could determine the details of the interlayered region of ZA-3. Thermal characteristics were determined with a thermogravimetric analysis (TGA) and differential scanning calorimetry (DSC), as shown in Figure 4b. The TG curve showed that 32 wt.% of ZA-3 was lost after heating to 800 °C through three stages. The first stage was 8 wt.% for removing the interlayered water and was accomplished at 173 °C. The second stage occurred at 316 °C for removing 18 wt.% of the interlayered anions. During the third stage, 6 wt.% was lost in the dehydroxylation process of the nanolayers. The DSC curve confirmed these three stages through three endothermic peaks at 153 °C, 211 °C, and 279 °C, as shown in Figure 4b.

The crystallite sizes of the particles of ZA-3, which were assessed from XRD peaks at widths of (003), (006), (009), and (015), were calculated to be 50 nm, 42 nm, 65 nm, and 40 nm, respectively. It means that the average particle size of ZA-3 was 49 nm. TEM images confirmed the nanoscale of sample ZA-3, as shown in Figure 5a,b. Figure 5a shows individual plates with thicknesses less than 50 nm. Figure 3 reveals that the shape of the particles looked like tapes with a width of 25 nm, as marked by arrows in the TEM images. The components of the nanolayers were identified using energy-dispersive X-ray spectrometry (EDX). Zinc, aluminum, oxygen, and carbon were observed in the EDX spectrum, as seen in Figure 5a (inset).

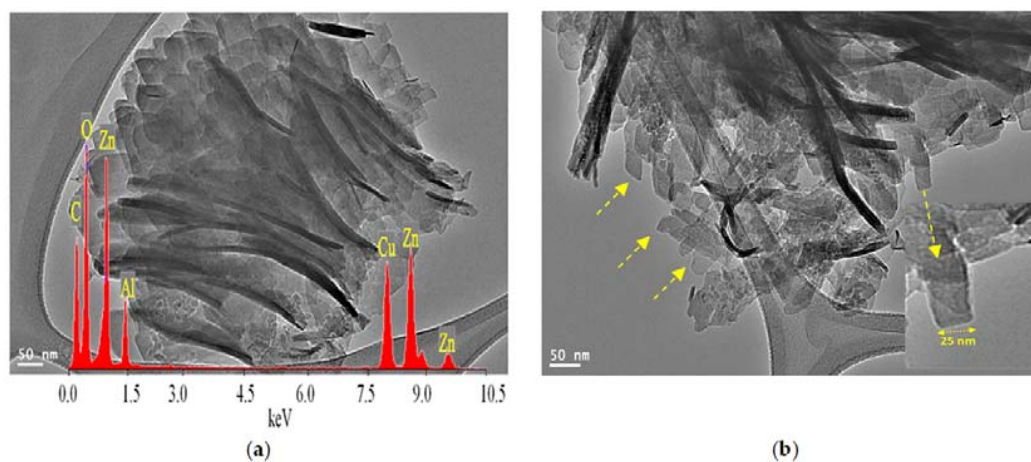


Figure 5. Sample ZA-3: (a) TEM images (inset: EDX spectrum) and (b) TEM images in another location.

X-ray diffraction, TEM, EDX, and thermal analyses concluded that the sample of ZA-3 consisted of nanotapes with nanolayers with a thickness of 0.48 nm connecting through pillars of carbonate anions and concentrating in the region of 0.274 nm between the nanolayers.

Compared with standard sample ZA-1, the nanolayered structure of ZA-3 could be more useful for removing heavy metals because sample ZA-3 had a smaller nanosize than ZA-1. It means that the number of entrance gates of heavy metals toward the interlayered regions of the nanolayered structures became higher, as shown in Figure 6.

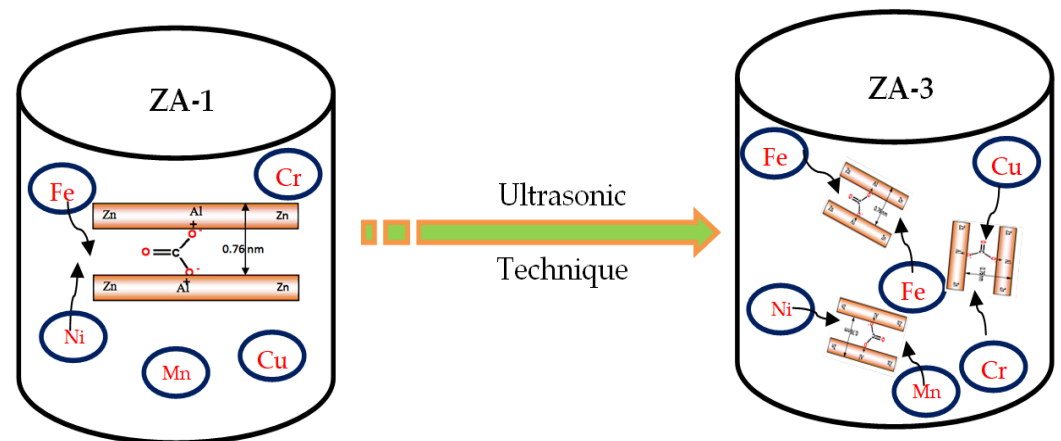


Figure 6. Adsorption process for purifying water from heavy metals at an extremely acidic medium for sample ZA-3 compared with standard sample ZA-1.

In this trend, sample ZA-3 was used for removing heavy metals (Fe, Cu, Cr, Ni, and Mn) from water through an adsorption process in an acidic medium. For Fe, high removal was observed, suggesting that sample ZA-3 was an effective material for purifying water, where the RE of Fe was 85%, as shown in Figure 7. This speculation was confirmed after removing the other heavy metals. The Cu and Cr removal percentages were 79% and 68%, respectively. In the case of the removal of Ni and Mn, the REs were 63% and 61%, respectively.

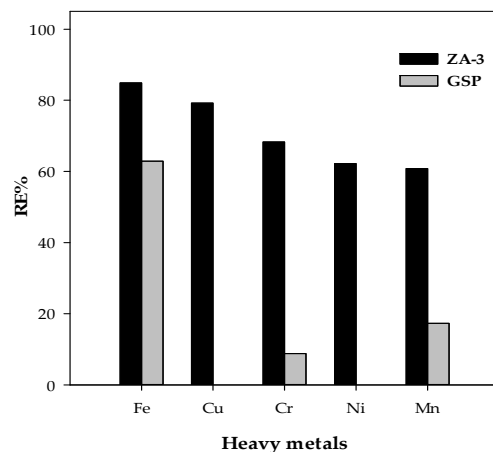


Figure 7. The removal percentages of heavy metals from water at an extremely acidic medium for samples ZA-3 and GSP.

By comparing with the results of Greensand Plus, Figure 7 confirms that sample ZA-3 was a good candidate as an efficient adsorbent for purifying water from heavy metals. Although the conditions of the adsorption process were severe, sample ZA-3 effectively removed Cu and Ni. However, Greensand Plus did not affect the removal of Cu and Ni. Additionally, the effect of sample ZA-3 on chromium was six times higher than that of

Greensand Plus. In addition, sample ZA-3 was about three times higher for the removal of manganese than Greensand Plus.

3.3. Antimicrobial Activity of Different Modified Al/Zn Nanolayered Structures

To determine the antimicrobial activities of prepared materials ZA-1, ZA-2, and ZA-3, a known concentration of the test samples was used after cultivation, and the subsequent incubation diameter of the inhibition zone was determined. The results presented in Table 2 indicate that ZA-1 had an inhibitory effect on the tested bacterial strain of *E. coli*, the most common coliform bacterium found in sewage wastewater, especially when dissolved in dimethyl sulfoxide (DMSO).

Table 2. Antimicrobial activity of prepared materials ZA-1, ZA-2, and ZA-3 against *E. coli*.

Diameter of Inhibition Zone (mm)					
Sample ZA-1		Sample ZA-2		Sample ZA-3	
D ¹	W	D	W	D	W
8.5	NA	11.3	10	18.5	NA

Notes: ¹ D: Zn-Al/LDH in dimethyl sulfoxide (DMSO); W: Zn-Al/LDH in water; NA: no inhibitory effect.

The major inhibitory effect of ZA-1 on *E. coli* was 8.5 mm. In concordance with this study, Moaty et al. [34] recorded that LDH exhibited long-lasting antimicrobial activity against fecal Gram-negative bacilli, including *E. coli*. The antibacterial effect of the nanolayered structure of ZA-1 could be explained through the adhesion process of microbial cells to the outer surface of the nanolayers of ZA-1 by van der Waals interaction and electrostatic exchanges [33]. The nanolayers were capable of interfering with microbial cells' division and growth. It was suggested that, in this scenario, DNA genetic material fail to replicate and cellular proteins become inactive [35].

The modification of LDH preparation using Zn/AL nitrate 15% (ZA-2) showed a limited increase in the activity of the nanomaterial. This increase was recorded when dissolved in water or DMSO, with inhibitory effects of approximately 10 mm and 11.3 mm, respectively.

It means that the growth of a new phase of zinc hydroxyl carbonate, in addition to LDH, caused an extra effect on the antimicrobial activity of LDH because sample ZA-2 consisted of two phases: a nanolayered structure of Al/Zn LDH and zinc hydroxyl carbonate. Therefore, a limited effect was observed on the antimicrobial activity of ZA-2.

Interestingly, the major antimicrobial activity was recorded when *E. coli* bacterial film was exposed to the nanolayered structure of ZA-3 (inhibition zone approximately 18.5 mm). This could be attributed to the smaller nanosize of sample ZA-3 compared to sample ZA-1 and the strong interaction between the surfaces of the bacterial cells and the nanolayer materials. On the other hand, the outer membrane of Gram-negative bacteria is well-known, e.g., *E. coli* has a vast number of hydrophilic transmembrane channel proteins called porins. These proteins form pores through the outer membrane, allowing hydrophilic molecules to diffuse into the periplasm [36]. Therefore, the hydrophilic nanoplates of ZA-3 could diffuse inside the periplasm and cause damage to the Gram-negative cell constituents, especially cell DNA genetic material.

Compared with the original sample of ZA-1, the activity of sample ZA-3 showed a potential antimicrobial effect against *E. coli*, a very familiar microbial contaminant in wastewater and sewage water. The inhibitory effect of ZA-3 was more than two-fold higher than that of ZA-1. Therefore, sample ZA-3 was considered a good candidate for treating wastewater and sewage water.

4. Discussion

The current study showed that the series of modifications used for developing the nanolayered structures of LDHs introduced new effective materials for work in severe conditions to purify water from different kinds of heavy metals and Gram-negative bacteria.

The ultrasonic technique was used for modifying the size of the platelets and the layers of LDHs to become nanosized and be more active in removing heavy metals under severe conditions with an antimicrobial effect.

Wang et al. [30] studied modified structures of LDHs based on a sulfide-selector intercalated layered double-hydroxide adsorbent for purifying water from only two metals (Cu and Mn) in normal conditions. Their results indicated that their materials were active for copper (100% removal) and inactive for manganese (0.66% removal). Our products were more effective compared with the results of Wang et al.

Recently, the application of LDHs for the elimination of some heavy metals, including Fe, Cu, and Cr ions, from the discharge of industrial wastewater was reported by Cardinale et al. [37]. In this work, two different LDH materials of MgAl-CO₃ and NiAl-NO₃ were fabricated to remove through adsorption some pollutants from the galvanic plant effluent described. Although there were high concentrations of Fe, Cu, and Cr ions in the original sample and a low pH value (3), the researchers adapted the experiment conditions to avoid severe conditions and decomposition of the synthesized materials by diluting the sample and raising the pH to 5. Interestingly, the NiAl-NO₃ LDH structure showed a higher affinity regarding Cr ions (almost 99%) than for Fe and Cu ions, which were 88% and 55%, respectively. In contrast, the MgAl-CO₃ LDH had a lower affinity to adsorb Cr ions (only 29%), whereas it was very powerful for the other two ions (almost 99%). By comparing the results of Cardinale et al. with the present work, the prepared materials resisted the high acidity of the medium (pH 2~3), as well as being able to treat Fe, Cu, and Cr ions with satisfactory removal efficiencies of 85%, 80%, and 70%, respectively. In addition, two more heavy metals were reasonably removed, where Ni and Mn ions were adsorbed with a removal efficiency of more than 60%, as well as the previously mentioned elements.

Asiabi et al. [29] studied the removal of copper y six samples for Ni-Cr LDHs. Although this study achieved an excellent removal percentage of Cu from the aqueous solution as an individual ion (almost 100%), this percentage did not exceed 31% during the adsorption of the best LDH structure (diphenylamine-4-sulfonate (DPA)) in the additional four different mixed ions (Cd, Cu, Zn, and Pb). In addition, the adsorption process was achieved under normal conditions (pH = 6).

The removal of Cr ions was performed by Tan et al. [38]. They concluded that CMC-LDH beads effectively removed a high concentration of Cr ions in an aqueous solution that was previously optimized according to pH in the range of 6–7. Although the adsorption ability of the studied material was powerful, the experimental conditions were adjusted for individual ideal Cr ion standard solutions. In other words, no competition was shown regarding the Cr ions studied with other types of heavy metals that may be found in real water or wastewater samples.

A study on an individual metal iron (II) removal from an aqueous solution was conducted by Taher et al. [39]. The results of this study proved that the elimination of Fe²⁺ using an intercalated Ca/Al LDH with Keggin ions was higher in adsorption capacity factor than the original Ca/Al LDH. Additionally, the stability and the highest adsorption capacity of the modified structures were diagnosed at a low pH, which is very similar to the current research findings. Another research output by Oktriyanti et al. [40] confirmed the power of modified structures of LDHs regarding the removal of iron from an aqueous solution in acidic conditions was more than pristine LDH.

It is rare to find an application of removing nickel ions using LDH. However, a recent study on the elimination of Ni²⁺ from water with nanoparticle structures (Fe/MoP) was discussed [39]. This study declared the removal of Ni ions only from water over 90% at the designed optimum conditions. These conditions were an alkaline medium (pH ~ 8), a temperature of 37 °C, and a contact time of 85 min.

Hence, the present modified structures prepared using the ultrasonic technique could be characterized as multi-ion selective materials working under nonoptimized severe conditions. Consequently, it is clear that, compared to the studies mentioned above, the current modified structures show multiple advantages. The first one is the ability to work

in severe conditions with a solid acidic medium. The second advantage is the ability to remove many heavy metals, including Fe, Cu, Cr, Ni, and Mn ions, from the same solution at the same time. In addition, a strong effect was observed against Gram-negative bacteria (*E. coli*) commonly found in wastewater.

5. Conclusions

In the current study, nanolayered structures of Al/Zn were prepared and developed through three methods to produce stable and strong structures for working in severe conditions to purify water from heavy metals and the most common Gram-negative bacterial pollutant, *E. coli*. Simultaneously, increasing their performance considered another target for the current study. Firstly, urea hydrolysis was used for preparing a standard, nanolayered structure of Al/Zn LDHs, which showed high activity for removing iron. However, lower activity was observed for the other metals: chromium, copper, nickel, and manganese. In addition, lower antimicrobial activity was observed. Decreasing the Al/Zn metal ratios of the nanolayered structure caused damage to 50% of the nanolayered structure. Accordingly, the activity decreased for removing the different types of heavy metals. At the same time, a limited increase was observed in the antimicrobial activity. The third method depended on the ultrasonic technique with urea hydrolysis, which improved the quality of the nanolayered structure by creating nanoplates and nanotapes of 25 nm in size. This technique increased the activity of the nanolayered structure to be very effective for removing different types of heavy metals because the nanosize of the particles increased the number of the entrance gates of heavy metals inside the interlayered region of the nanolayered structures. In the same trend, strong activity against Gram-negative bacteria (*E. coli*) commonly found in wastewater was observed. In this way, the activity of the nanolayered structures was very high for removing different kinds of heavy metals from water, in addition to the purification of water from Gram-negative bacteria.

Finally, these experimental results concluded that the nanolayered structures based on the ultrasonic technique could be considered multifunctional materials. It showed effective results for removing different kinds of heavy metals in severe conditions and introduced new, promising materials for purifying industrial water that has a very acidic medium. In addition, it can be used for treating wastewater because of its strong activity against Gram-negative bacteria (*E. coli*) that are commonly found in wastewater.

Author Contributions: Conceptualization, A.A.A., O.S. and M.F.E.; methodology, A.A.A., O.S., M.M.B. and W.I.M.E.-A.; software, A.A.A. and W.I.M.E.-A.; validation, A.A.A., M.F.E. and M.M.B.; formal analysis, W.I.M.E.-A.; investigation, A.A.A., M.F.E. and M.M.B.; writing—original draft preparation, A.A.A., O.S., M.F.E. and M.M.B.; writing—review and editing, A.A.A., M.F.E. and M.M.B.; All authors have read and agreed to the published version of the manuscript.

Funding: This research was funded by the Deanship of Scientific Research, Imam Abdulrahman Bin Faisal University (IAU), Saudi Arabia (grant number 2019-018-CPH), and the APC was funded by 2019-018-CPH.

Institutional Review Board Statement: Not applicable.

Informed Consent Statement: Not applicable.

Data Availability Statement: Not applicable.

Acknowledgments: The authors acknowledge the financial support from the Deanship of Scientific Research (DSR), Imam Abdulrahman Bin Faisal University (IAU), Saudi Arabia (Grant Application No. 2019-018-CPH). Special appreciation is extended to King Faisal University for the facilities and the technical support.

Conflicts of Interest: The authors declare no conflict of interest.

References

1. Gorzin, F.; Bahri Rasht Abadi, M.M. Adsorption of Cr(VI) from Aqueous Solution by Adsorbent Prepared from Paper Mill Sludge: Kinetics and Thermodynamics Studies. *Adsorpt. Sci. Technol.* **2018**, *36*, 149–169. [[CrossRef](#)]

2. Madhavi, A.; Srinivasulu, M.; Chandra, M.S.; Rangaswamy, V. Detoxification of Heavy Metals Using Marine Metal Resistant Bacteria: A New Method for the Bioremediation of Contaminated Alkaline Environments. In *Innovations Biotechnology Sustainable Future*; Springer: Cham, Switzerland, 2021; pp. 297–332. [[CrossRef](#)]
3. Acrylamide, O.C. National Primary Drinking Water Regulations. *Kidney* **2009**, *2*, 9.
4. US EPA. National Primary Drinking Water Regulations. 2022. Available online: <https://www.epa.gov/ground-water-and-drinking-water/national-primary-drinking-water-regulations> (accessed on 22 February 2022).
5. AlMulla, A. Understanding the Impacts of Changing Soil Temperature, Water Irrigation Source and Fertiliser Types on C and N Cycling in Arid Soils. Ph.D. Thesis, Bangor University, Bangor, UK, 2016.
6. Rajaiitha, P.M.; Hajra, S.; Sahu, M.; Mistewicz, K.; Toróñ, B.; Abolhassani, R.; Panda, S.; Mishra, Y.K.; Kim, H.J. Unraveling Highly Efficient Nanomaterial Photocatalyst for Pollutant Removal: A Comprehensive Review and Future Progress. *Mater. Today Chem.* **2022**, *23*, 100692. [[CrossRef](#)]
7. Gómez-López, P.; Puente-Santiago, A.; Castro-Beltrán, A.; Santos do Nascimento, L.A.; Balu, A.M.; Luque, R.; Alvarado-Beltrán, C.G. Nanomaterials and Catalysis for Green Chemistry. *Curr. Opin. Green Sustain. Chem.* **2020**, *24*, 48–55. [[CrossRef](#)]
8. Liang, X.J.; Kumar, A.; Shi, D.; Cui, D. Nanostructures for Medicine and Pharmaceuticals. *J. Nanomater.* **2012**, *2012*, 921897. [[CrossRef](#)]
9. Kusior, A.; Klich-Kafel, J.; Trenczek-Zajac, A.; Swierczek, K.; Radecka, M.; Zakrzewska, K. TiO₂-SnO₂ Nanomaterials for Gas Sensing and Photocatalysis. *J. Eur. Ceram. Soc.* **2013**, *33*, 2285–2290. [[CrossRef](#)]
10. Ajayi, R.F.; Barry, S.; Nkuna, M.; Ndou, N.; Rakgotho, T.; Nqunqa, S.; Ngema, N.; Thipe, V.; Muluadzi, T. Nanoparticles in Biosensor Development for the Detection of Pathogenic Bacteria in Water. *Emerging Freshwater Pollutants* **2022**, 331–358. [[CrossRef](#)]
11. Das, R.; Vecitis, C.D.; Schulze, A.; Cao, B.; Ismail, A.F.; Lu, X.; Chen, J.; Ramakrishna, S. Recent Advances in Nanomaterials for Water Protection and Monitoring. *Chem. Soc. Rev.* **2017**, *46*, 6946–7020. [[CrossRef](#)]
12. Lu, H.; Wang, J.; Stoller, M.; Wang, T.; Bao, Y.; Hao, H. An Overview of Nanomaterials for Water and Wastewater Treatment. *Adv. Mater. Sci. Eng.* **2016**, *2016*, 4964828. [[CrossRef](#)]
13. Baby, R.; Hussein, M.Z.; Abdullah, A.H.; Zainal, Z. Nanomaterials for the Treatment of Heavy Metal Contaminated Water. *Polymers* **2022**, *14*, 583. [[CrossRef](#)]
14. Saber, O.; Shaalan, N.M.; Ahmed, F.; Kumar, S.; Alshoaibi, A. One-Step Multi-Doping Process for Producing Effective Zinc Oxide Nanofibers to Remove Industrial Pollutants Using Sunlight. *Crystals* **2021**, *11*, 1268. [[CrossRef](#)]
15. Saber, O.; Asiri, S.M.; Ezzeldin, M.F.; El-Azab, W.I.M.; Abu-Abdeen, M. Designing Dual-Effect Nanohybrids for Removing Heavy Metals and Different Kinds of Anions from the Naturalwater. *Materials* **2020**, *13*, 2524. [[CrossRef](#)]
16. Das, S.; Chakraborty, J.; Chatterjee, S.; Kumar, H. Prospects of Biosynthesized Nanomaterials for the Remediation of Organic and Inorganic Environmental Contaminants. *Environ. Sci. Nano* **2018**, *5*, 2784–2808. [[CrossRef](#)]
17. dos Santos Ramos, M.A.; de Toledo, L.G.; Spósito, L.; Marena, G.D.; de Lima, L.C.; Fortunato, G.C.; Araújo, V.H.S.; Bauab, T.M.; Chorilli, M. Nanotechnology-Based Lipid Systems Applied to Resistant Bacterial Control: A Review of Their Use in the Past Two Decades. *Int. J. Pharm.* **2021**, *603*, 120706. [[CrossRef](#)] [[PubMed](#)]
18. Mishra, G.; Dash, B.; Pandey, S. Layered Double Hydroxides: A Brief Review from Fundamentals to Application as Evolving Biomaterials. *Appl. Clay Sci.* **2018**, *153*, 172–186. [[CrossRef](#)]
19. Bezerra, D.M.; Rodrigues, J.E.F.S.; Assaf, E.M. Structural, Vibrational and Morphological Properties of Layered Double Hydroxides Containing Ni²⁺, Zn²⁺, Al³⁺ and Zr⁴⁺ Cations. *Mater. Charact.* **2017**, *125*, 29–36. [[CrossRef](#)]
20. Mallakpour, S.; Hatami, M.; Hussain, C.M. Recent Innovations in Functionalized Layered Double Hydroxides: Fabrication, Characterization, and Industrial Applications. *Adv. Colloid Interface Sci.* **2020**, *283*, 102216. [[CrossRef](#)]
21. Chubar, N.; Gilmour, R.; Gerda, V.; Mičušík, M.; Omastova, M.; Heister, K.; Man, P.; Fraissard, J.; Zaitsev, V. Layered Double Hydroxides as the next Generation Inorganic Anion Exchangers: Synthetic Methods versus Applicability. *Adv. Colloid Interface Sci.* **2017**, *245*, 62–80. [[CrossRef](#)]
22. Mallakpour, S.; Dinari, M.; Hatami, M. Novel Nanocomposites of Poly(Vinyl Alcohol) and Mg-Al Layered Double Hydroxide Intercalated with Diacid N-Tetrabromophthaloyl-Aspartic: Optical, Thermal and Mechanical Properties. *J. Therm. Anal. Calorim.* **2015**, *120*, 1293–1302. [[CrossRef](#)]
23. Baruah, A.; Mondal, S.; Sahoo, L.; Gautam, U.K. Ni-Fe-Layered Double Hydroxide/N-Doped Graphene Oxide Nanocomposite for the Highly Efficient Removal of Pb(II) and Cd(II) Ions from Water. *J. Solid State Chem.* **2019**, *280*, 120963. [[CrossRef](#)]
24. Liu, S.Q.; Li, S.P.; Li, X.D. Intercalation of Methotrexatum into Layered Double Hydroxides via Exfoliation-Reassembly Process. *Appl. Surf. Sci.* **2015**, *330*, 253–261. [[CrossRef](#)]
25. Sanati, S.; Rezvani, Z. Ultrasound-Assisted Synthesis of NiFe- Layered Double Hydroxides as Efficient Electrode Materials in Supercapacitors. *Ultrason. Sonochem.* **2018**, *48*, 199–206. [[CrossRef](#)] [[PubMed](#)]
26. Althabaiti, N.S.; Al-Nwaiser, F.M.; Saleh, T.S.; Mokhtar, M. Ultrasonic-Assisted Michael Addition of Arylhalide to Activated Olefins Utilizing Nanosized Comgal-Layered Double Hydroxide Catalysts. *Catalysts* **2020**, *10*, 220. [[CrossRef](#)]
27. Grover, A.; Mohiuddin, I.; Malik, A.K.; Aulakh, J.S.; Kim, K.H. Zn-Al Layered Double Hydroxides Intercalated with Surfactant: Synthesis and Applications for Efficient Removal of Organic Dyes. *J. Clean. Prod.* **2019**, *240*, 118090. [[CrossRef](#)]
28. Shamsayei, M.; Yamini, Y.; Asiabi, H. Fabrication of Zwitterionic Histidine/Layered Double Hydroxide Hybrid Nanosheets for Highly Efficient and Fast Removal of Anionic Dyes. *J. Colloid Interface Sci.* **2018**, *529*, 255–264. [[CrossRef](#)] [[PubMed](#)]

29. Asiabi, H.; Yamini, Y.; Shamsayei, M.; Tahmasebi, E. Highly Selective and Efficient Removal and Extraction of Heavy Metals by Layered Double Hydroxides Intercalated with the Diphenylamine-4-Sulfonate: A Comparative Study. *Chem. Eng. J.* **2017**, *323*, 212–223. [[CrossRef](#)]
30. Wang, J.; Zhang, L.; Zhang, T.; Du, T.; Li, T.; Yue, T.; Li, Z.; Wang, J. Selective Removal of Heavy Metal Ions in Aqueous Solutions by Sulfide-Selector Intercalated Layered Double Hydroxide Adsorbent. *J. Mater. Sci. Technol.* **2019**, *35*, 1809–1816. [[CrossRef](#)]
31. Duan, S.; Ma, W.; Cheng, Z.; Zong, P.; Sha, X.; Meng, F. Preparation of Modified Mg/Al Layered Double Hydroxide in Saccharide System and Its Application to Remove As(V) from Glucose Solution. *Colloids Surf. Physicochem. Eng. Asp.* **2016**, *490*, 250–257. [[CrossRef](#)]
32. Bauer, A.W. Antibiotic Susceptibility Testing by a Standardized Single Disc Method. *Am. J. Clin. Pathol.* **1966**, *45*, 149–158. [[CrossRef](#)]
33. Faille, C.; Jullien, C.; Fontaine, F.; Bellon-Fontaine, M.N.; Slomianny, C.; Benezech, T. Adhesion of Bacillus Spores and Escherichia Coli Cells to Inert Surfaces: Role of Surface Hydrophobicity. *Can. J. Microbiol.* **2002**, *48*, 728–738. [[CrossRef](#)]
34. Moaty, S.A.A.; Farghali, A.A.; Khaled, R. Preparation, Characterization and Antimicrobial Applications of Zn-Fe LDH against MRSA. *Mater. Sci. Eng. C* **2016**, *68*, 184–193. [[CrossRef](#)] [[PubMed](#)]
35. Youssef, A.M.; Moustafa, H.; Barhoum, A.; Hakim, A.E.F.A.A.; Dufresne, A. Evaluation of the Morphological, Electrical and Antibacterial Properties of Polyaniline Nanocomposite Based on Zn/Al-Layered Double Hydroxides. *ChemistrySelect* **2017**, *2*, 8553–8566. [[CrossRef](#)]
36. Donev, R. *Advances in Protein Chemistry and Structural Biology*; Academic Press: Cambridge, MA, USA, 2014.
37. Cardinale, A.M.; Carbone, C.; Consani, S.; Fortunato, M.; Parodi, N. Layered Double Hydroxides for Remediation of Industrial Wastewater from a Galvanic Plant. *Crystals* **2020**, *10*, 443. [[CrossRef](#)]
38. Tan, L.; Li, H.; Liu, M. Characterization of CMC-LDH Beads and Their Application in the Removal of Cr(vi) from Aqueous Solution. *RSC Adv.* **2018**, *8*, 12870–12878. [[CrossRef](#)] [[PubMed](#)]
39. Taher, T.; Christina, M.M.; Said, M.; Hidayati, N.; Ferlinahayati, F.; Lesbani, A. Removal of Iron(II) Using Intercalated Ca/Al Layered Double Hydroxides with $[\alpha\text{-SiW}_{12}\text{O}_{40}]^{4-}$. *Bull. Chem. React. Eng. Catal.* **2019**, *14*, 260–267. [[CrossRef](#)]
40. Oktriyanti, M.; Palapa, N.R.; Mohadi, R.; Lesbani, A. Effective Removal of Iron (II) from Aqueous Solution by Adsorption Using Zn/Cr Layered Double Hydroxides Intercalated with Keggin Ion. *J. Ecol. Eng.* **2020**, *21*, 63–71. [[CrossRef](#)]